

# MR CISS (Constructive Interference in Steady State)

1

1,2

1,2

CISS (Constructive Interference in Steady State)

MRI

1.5 T MR : MRI T2 20 2D FLASH CISS

, CISS . CISS CISS

CISS (n=17) CISS (n=5) 90%

CISS (n=15) 가 CISS (n=7), (n=20) (n=4) CISS 가 가

: CISS 가 CISS MRI

가 CT, MRI, (MR myelography) MRI

가 (1, 2). (brachial plexus) (6,7). 3D FT (Three Dimensional Fourier Trans- formation) CISS MRI

MRI 가 CT- (3-5). (8,9), 1-2mm 3D FT CISS MRI

가 3D FT CISS MRI 가

1  
2  
1998 11 4 1999 3 6

1998 3 7  
 20  
 7  
 18 71 45 13  
 15 ( 15 5 )  
 2 1 2  
 1.5 T MRI (Vision plus,  
 Siemens, Erlangen, Germany)  
 T2, 2D FLASH  
 3D FT CISS 가  
 T2 (repetition  
 time) [TR] / (echo time) [TE] / flip angle (FA)  
 4700 msec/ 112 msec/ 180, 2D FLASH  
 920 msec/ 22 msec/ 30, 3D FT CISS  
 TR/TE/FA 12.25/5.9/70  
 224 × 226, slab 64mm, field of view (FOV)  
 200mm, 1mm, (NEX) 1  
 CP neck array coil  
 3D FT CISS 3  
 45  
 가 ( CISS )  
 가 MR  
 2  
 가

CISS  
 2D FLASH CISS  
 가 CISS  
 가  
 Cochran's Q test 95%  
 2  
 CISS ( T2  
 2D FLASH ) 가  
 Table 1-3 가  
 가  
 5 90% (4.5/5, 90%) CISS  
 (n=5) (n=4)  
 CT (n=2)  
 (Fig. 1A, B)  
 15 가  
 CISS 3  
 45  
 가

Table 1. Comparison of CISS and Conventional MR Sequences by Two Readers in Evaluation of Neural Foramen Stenosis.

Readers	CISS> Conventional	CISS= Conventional	CISS< Conventional
1	5/5 (100%)	0/5	0/5
2	4/5 (80%)	1/5 (20%)	0/5
mean	4.5/5 (90%)	0.5/5 (10%)	0/5

CISS: Constructive interference in steady state

Table 2. Comparison of CISS and Conventional MR Sequences by Two Readers in Visualization of Nerve Roots.

Readers	CISS> Conventional	CISS= Conventional	CISS< Conventional
1	18/20 (90%)	2/20 (10%)	-
2	16/20 (80%)	2/20 (10%)	2*/20 (10%)
mean	17/20 (85%)	2/20 (10%)	1/20 (5%)

CISS : Constructive interference in steady state

\* : Patients with infectious spondylitis or severe HIVD (herniated intervertebral disc)

Table 3. Comparison of CISS and Conventional MR Sequences for Evaluation of Other Five Criterion of Cervical Spinal Diseases.

	CISS> Conventional	CISS= Conventional	CISS< Conventional
Contrast between CSF/tissues	15/20 (75%)	5/20 (25%)	0/20
Diagnosis of HIVD (N= 15)	0/15	15/15 (100%)	0/15
Characterization of herniated disc	0/15	8/15 (53%)	7/15 (47%)
Delineation of intramedullary lesion* (N= 4 <sup>†</sup> )	0/4	0/4	4/4 (100%)
Contrast of gray-white matter	0/20	0/20	20/20 (100%)

CISS: Constructive interference in steady state

HIVD: Herniated intervertebral disc

\*: Comparison with turbo spin echo T2 weighted sagittal image

†: Compressive myelopathy

> : better than, = : equal to

Interest: ROI) 가 (Region of compressive myelopathy) 3 (compress-  
 (Fig. 1C). T2 CISS 가  
 17 (17/20, 85%) CISS (Fig. 2, 3), 20 (20/20, 100%) CISS (Fig. 5).  
 (Fig. 2C). 1 CISS 75% (15/20)  
 CISS 가  
 15 MRI 가  
 7 CISS (Fig. 4).

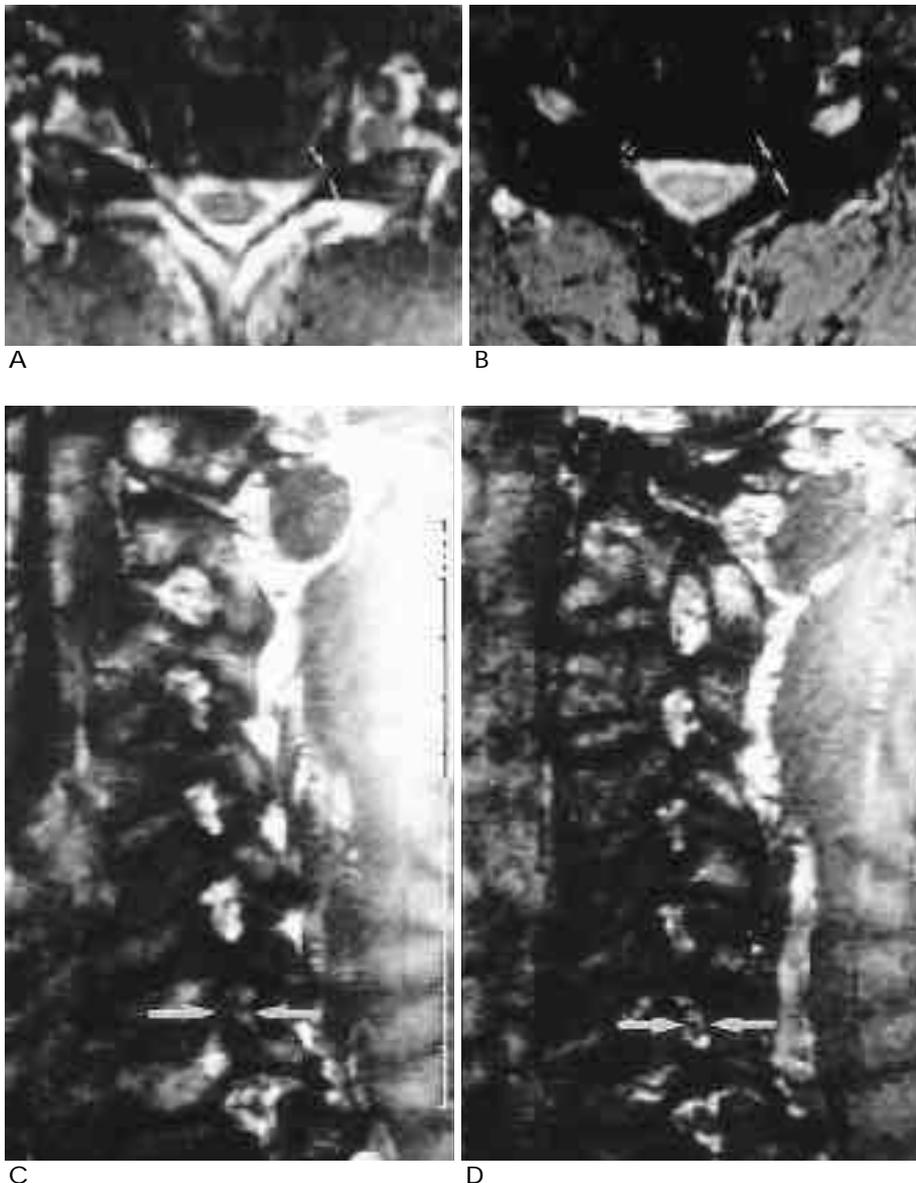


Fig. 1. Neural foramen stenosis in a 63-year-old woman with radicular pain in the left shoulder.  
 A. CISS reformatted axial image shows narrowing of left (white arrows) and intact right (small double arrows) C6-C7 neural foramen.  
 B. 2D FLASH image shows neural foramen stenosis in left (white arrows) and suspicious stenosis in right (small double arrows) C6-C7 level.  
 C. CISS reformatted left oblique coronal image reveals narrowing of the left neural foramen (arrows) at C6-C7.  
 D. CISS reformatted right oblique coronal image shows the intact right neural foramen at C4-C5, C5-C6 and C6-C7 (arrows). Neural foramen of entire cervical vertebrae can be readily evaluated at a glance on oblique coronal views.

가 : MR Constructive Interference in Steady State  
 가 가 MRI CT- MRI Gustavo CT-  
 가 MRI CT- MRI 85% (3)  
 45-100% 6-70% 52% MR

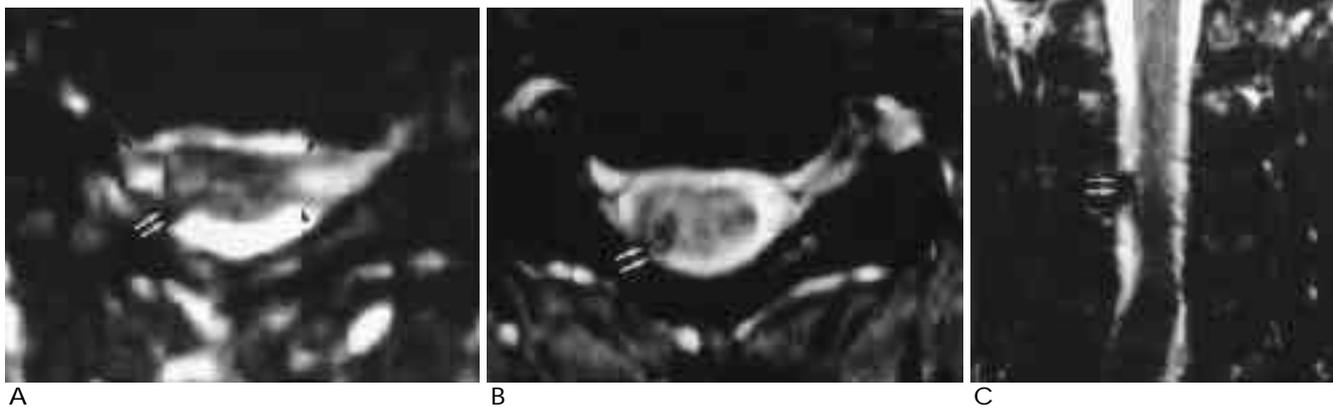


Fig. 2. Brachial plexus injury in an 18-year-old man with weakness of right arm.  
 A. CISS axial image shows a focal lesion of low signal intensity suggesting fibrotic scar tissue (double arrows) at the junction of spinal cord and dorsal rootlet. Note the intact ventral and dorsal rootlets on the both sides (arrowheads).  
 B. 2D FLASH axial image shows a similar lesion of low intensity at the same area (double arrows).  
 C. CISS coronal image displays the single lesion of low intensity at the area of C5 dorsal rootlet (double arrows) and intact rootlets of other levels.

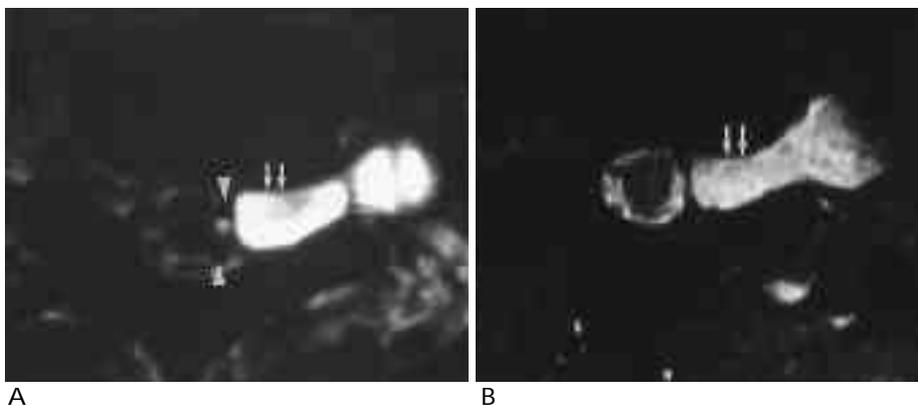


Fig. 3. Brachial plexus injury in a 23-year-old man with paresis of left arm.  
 A. CISS axial image at the level of T1-T2 reveals post-traumatic pseudomeningocele (double arrows) at the left neural foramen and extraforaminal area. But, the ventral and dorsal rootlets (arrowheads) appear to be intact.  
 B. 2D FLASH axial image reveals similar finding of the pseudomeningocele (double arrows), but the ventral and dorsal rootlets are not well delineated.

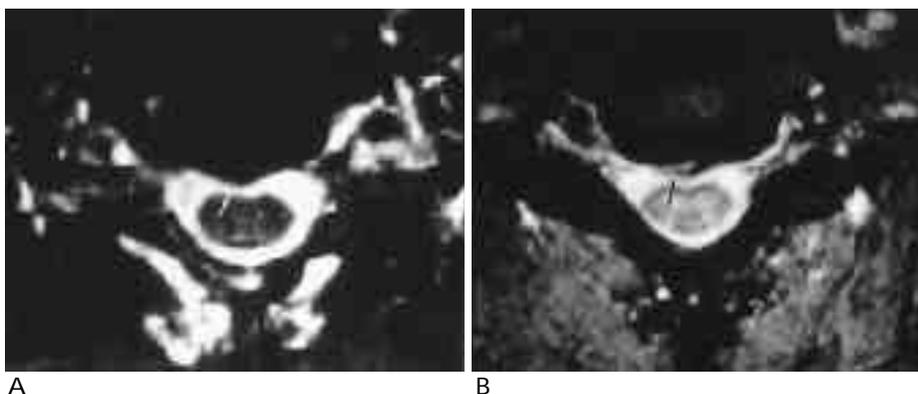


Fig. 4. Intervertebral soft disc herniation at C5-C6 in a 57-year-old man.  
 A. CISS axial image shows a focal central protrusion of low signal intensity (arrow) indenting ventral subarachnoid space. It is not possible to differentiate soft disc protrusion from osteophyte.  
 B. 2D FLASH axial image shows that the focal protrusion has high signal intensity indicating soft disc protrusion, but not osteophyte (arrow).



Fig. 5. Presumed cord edema in a 45-year-old man with infectious spondylitis and its epidural extension  
 A. CISS coronal image shows subtle high signal intensity within the upper cervical cord (arrow).  
 B. Fast spin echo T2-weighted sagittal image shows that the high signal intensity within the high cervical cord is more conspicuous (arrow). Note the infectious spondylitis with abscess extending into prevertebral and postvertebral spaces in C5-6 level.

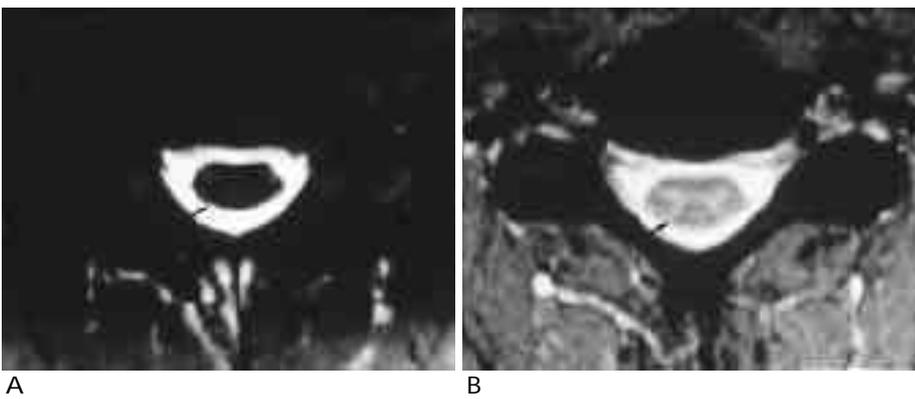


Fig. 6. Contrast between normal gray and white matters  
 A. CISS axial image shows poor contrast between normal gray and white matters (arrow).  
 B. 2D FLASH axial image shows better contrast between normal gray and white matters (arrow).

MR 가 가  
 (3). slice 3-5mm MRI가 가  
 가 , 가  
 3mm (3, 11).  
 3mm  
 (gradient echo) 2D FLASH 가 (12). 2D FLASH 가 3mm  
 2D FLASH 가  
 flip angle 50-60 가  
 10 flip angle (10). CISS 0.5mm  
 30 flip angle  
 1.5-3mm (8, 9), CISS  
 가

가

CISS 3DFT T2  
 (Heavily T2-weighted image) true FISP (Fast Imaging  
 in Steady state Precession) (13-16) MR  
 (8, 9). FISP  
 가

CISS C1 C7

2D FLASH  
 CISS

(17). True FISP Cassleman (8)

FISP PSIF (reversed FISP)

CISS

FISP (18).  
 true FISP osteophyte

FISP PSIF가  
 (band artifact)  
 alternating (+/-) RF pulse nonalternating (+/+) RF pulse  
 가 true FISP

2D FLASH

CISS (8).  
 CISS 2D FLASH 가  
 가 2D FLASH 2

가 (17/20, 85%). 가 CISS

MRI 가 CISS  
 가 가

T2 가  
 (Fig. 2A, B). FLASH CISS T2 2D  
 5 CISS

CISS

(ROI) 가 MRI CISS  
 MRI (Fig. 2C). 가

Blum (5)

가  
 (3, 19-22).

T1-T2 CISS  
 2D FLASH  
 (Fig. 3A, B)

가 CISS

5 Tsuruda (23)  
 phantom MRI

1. Berns DH, Blaser SI, Modic MT. Magnetic resonance imaging of the spine. *Clin Orthop* 1989 ;(244):78-100
2. Hyman RA, Edwards JH, Vacirca SJ, Stein HL. 0.6 T MR imaging of the cervical spine: multislice and multiecho techniques. *AJNR* 1985 ;6(2):229-3
3. Carvalho GA, Nikkhah G, Matthies C, Penkert G, Samii M. Diagnosis of root avulsions in traumatic brachial plexus injuries: value of computerized tomography myelography and magnetic resonance imaging. *J Neurosurg* 1997;86(1):69-76
4. Volle E, Assheuer J, Hedde JP, Gustorf-Aeckerle R. Radicular avulsion resulting from spinal injury: assessment of diagnostic modalities. *Neuroradiology* 1992;34(3):235-40
5. Blum U, Friedburg HG, Ott D, Wimmer B. Traction injuries of the brachial plexus: radiologic diagnosis using myelo-CT and MR. *Rofu Fortschr Geb Rontgenstr Neuen Bildgeb Verfahr* 1989;151(6):702-5

- [Article in German]
6. Hofman PA, Wilmink JT. Optimising the image of the intradural nerve root: the value of MR radiculography. *Neuroradiology* 1996;38(7):654-7
  7. VanDyke CW, Modic MT, Beale SM, Amartur S, Ross JS. 3D MR myelography. *J Comput Assist Tomogr* 1992;16(3):497-500
  8. Casselman JW, Kuhweide R, Deimling M, Ampe W, Dehaene I, Meeus L. Constructive interference in steady state-3DFT MR imaging of the inner ear and cerebellopontine angle. *AJNR* 1993;14(1):47-57
  9. Casselman JW, Kuhweide R, Dehaene I, Ampe W, Devlies F. Magnetic resonance examination of the inner ear and cerebellopontine angle in patients with vertigo and/or abnormal findings at vestibular testing. *Acta Otolaryngol Suppl* (Stockh) 1994;513:15-27
  10. Schubeus P, Sander B, Schorner W, Tosch U, Lanksch WR, Felix R. MRI of the cervical spine using T1-weighted multislice FLASH sequences. *Rofu Fortschr Geb Rontgenstr Neuen Bildgeb Verfahr* 1990 ;153(4):461-6. [Article in German]
  11. Georgy BA, Hesselink JR. MR imaging of the spine: recent advances in pulse sequences and special techniques. *AJR* 1994;162(4):923-34
  12. Som PM, Curtin HD. *Head and Neck Imaging*, 3rd ed. St.Louis: Mosby, 1996:1010-1011
  13. Oppelt A, Groumann R, Varfuss H, Fisher H, Harh W, Schajar W. FISP, a new fast MRI sequence. *Electromedica* 1986;54:15-18
  14. Gyngell ML. The application of steady-state free precession in rapid 2DFT NMR imaging: FAST and CE-FAST sequences. *Magn Reson Imaging* 1988;6(4):415-9
  15. Nakamura H, Murakami T, Ishida T, et al. 3DFT-FISP MRI with gadopentetate dimeglumine in differential diagnosis of small liver tumors. *J Comput Assist Tomogr* 1994;18(1):49-54
  16. Sakamoto Y, Takahashi M, Ushio Y, Korogi Y. Visibility of epidermoid tumors on steady-state free precession images. *AJNR* 1994;15(9):1737-44
  17. Price RR. The AAPM/RSNA physics tutorial for residents. Contrast mechanisms in gradient-echo imaging and an introduction to fast imaging. *RadioGraphics* 1995;15(1):165-78
  18. Edelman RR, Hesselink JR, Elatkin MB. *Clinical Magnetic resonance imaging*, 2nd ed. Philadelphia:Saunders 1996:302-324
  19. Yeoman PM. Cervical myelography in traction injuries of the brachial plexus. *J Bone Joint Surg [Br]* 1968;50(2):253-60
  20. Piegras U, Jelasic F, Kammerer V, Traupe H. Radiologische Befund bei zervikaren Wurzelaustrissen. *Radiology* 175;15:317-322
  21. de Verdier HJ, Colletti PM, Terk MR. MRI of the brachial plexus: a review of 51 cases. *Comput Med Imaging Graph* 1993;17(1):45-50
  22. Roger B, Delmas PF, Chaise F, Sedel L, Laval-Jeantet M, Fria J. Cervical myelography and x-ray computed tomography in arm paralysis of traumatic origin. *J Radiol* 1985;66(11):659-66 [Article in French]
  23. Tsuruda JS, Remley K. Effects of magnetic susceptibility artifacts and motion in evaluating the cervical neural foramina on 3DFT gradient-echo MR imaging. *AJNR* 1991;12(2):237-41

## Usefulness of 3D CISS Sequence in MR Imaging of Cervical Spine<sup>1</sup>

Se Hyung Kim, M.D., Kee-Hyun Chang, M.D.<sup>1,2</sup>, Jin Mo Goo, M.D., Sung Ho Park, M.D.,  
Chang Gyu Sung, M.D., Jin Il Jung, M.D., Hong Dae Kim, M.D., Moon Hee Han, M.D.<sup>1,2</sup>

<sup>1</sup>Department of Radiology, Seoul National University College of Medicine,

<sup>2</sup>Department of Institute of Radiation Medicine, SNUMRC

**Purpose :** To assess the value of 3D CISS (constructive interference in steady state) MR sequence in imaging the cervical spine.

**Materials and Methods :** MR images of cervical spine were prospectively obtained with both conventional (sagittal TSE and axial 2D FLASH) and CISS sequences in 20 patients suspected of having cervical spinal diseases. MR technique was performed on a 1.5T MR machine.

Axial, oblique coronal, and curved coronal images were reformatted with the 3D raw datas of CISS sequence which were obtained in coronal plane. The findings of CISS sequence were compared with those of the conventional sequence in terms of visualization of the neural foramen and nerve roots, detection and differentiation of herniated disc, conspicuity of the intramedullary lesion, contrast between the CSF and spinal cord and between the gray and white matters within the cord.

**Results :** In 17 cases including traumatic root avulsions, 3D CISS sequence demonstrated the intradural nerve roots with excellent contrast especially in coronal plane. Reformatted oblique coronal images of CISS sequence offered better visualization of entire neural foramen beyond the region of interest. CISS sequence was superior to the conventional sequence in demonstration of disease extent and correlation to the clinical symptoms in 4.5 cases of foraminal stenosis and in contrast between the CSF and spinal cord (n= 15). CISS sequence was almost equal to the conventional sequence in detection of herniated disc (n= 15). CISS was inferior to the conventional sequence in differentiation of herniated disc (n= 7), delineation of intramedullary lesion (n= 4) and in contrast between the gray and white matter within the cord in all patients.

**Conclusion :** The 3D CISS sequence gives better information than the conventional sequence especially in the evaluation of the nerve roots and neural foramens but worse contrast of intramedullary lesion. It may well be used as a supplementary sequence in assessment of foraminal stenosis and nerve root injury.

**Index words :** Cervical spine, MR

Magnetic resonance (MR), technology

Magnetic resonance (MR), three-dimensional

Address reprint requests to : Kee-Hyun Chang, M.D., Department of Radiology, Seoul National University College of Medicine  
#28, Yongon-dong, Chongno-gu, Seoul, 110-744, Korea.  
Tel. 82-2-760-2584 Fax. 82-2-743-6385